

1 Abstract

2 Taxonomic diversity effects on forest productivity and response to climate extremes range from
3 positive to negative, suggesting a key role for complex interactions among neighbouring trees.
4 To elucidate how neutral interactions, hierarchical competition and resource partitioning between
5 neighbours shape tree growth and climate response in a highly diverse Amazonian forest, we com-
6 bined 30 years of tree censuses with measurements of water and carbon related traits. We modelled
7 individual tree growth response to climate and neighbourhood to disentangle the relative effect
8 of neighbourhood densities, trait hierarchies and dissimilarities. While neighbourhood densities
9 consistently decreased tree growth, trait dissimilarity increased it, and both influenced climate
10 response. Greater water conservatism provided a competitive advantage to focal trees in normal
11 years, but water spender neighbours reduced this effect in dry years. By underlining the impor-
12 tance of density and trait-mediated neighbourhood interactions, our study offers a way towards
13 improving predictions of forest response to climate change.

¹⁴ Introduction

¹⁵ Climate extremes such as heat waves, high atmospheric evaporative demands and low soil water
¹⁶ availability (i.e drought stress sensu lato), negatively affect forest productivity and functioning
¹⁷ (Allen *et al.*, 2010; Bauman *et al.*, 2022a,b). These events are predicted to increase in frequency
¹⁸ and intensity with ongoing climate change (Shukla *et al.*, 2022), which can alter global carbon
¹⁹ dynamics (Higgins *et al.*, 2023). At the global scale, tree taxonomic diversity is an important driver
²⁰ of forest productivity (Liang *et al.*, 2016), and can increase forest resistance to drought (Anderegg
²¹ *et al.*, 2018). However, at local scales, the magnitude and even the sign of the effect of diversity on
²² productivity can vary from site to site, depending on the local context (e.g. climate and disturbance
²³ regimes, stand structure and composition: Ammer 2019; Belote *et al.* 2011; Crawford *et al.* 2021)
²⁴ and temporal variations in resource availability or climate (Forrester & Bauhus, 2016). Increasing
²⁵ evidence further suggests that diversity does not always increase forest resistance to droughts
²⁶ locally (Grossiord, 2020; Pardos *et al.*, 2021). Uncovering the mechanisms that underlie diversity
²⁷ effects on forest productivity and its response to climate is needed to better understand these
²⁸ context-dependent effects (Grossiord, 2020) and improve our ability to predict forest responses to
²⁹ climate change.

³⁰ Complementarity in resource use among co-occurring species has been proposed to explain in-
³¹ creased forest productivity (Liang *et al.*, 2015; Morin *et al.*, 2011) and resistance to environmental
³² fluctuations, such as climate extremes (Loreau & de Mazancourt, 2013) in species diverse stands.
³³ As competition for resources takes place at the neighbourhood scale, evidence for such an effect
³⁴ and its signature should be found in the influence of neighbours' identity on individual tree growth
³⁵ (Yu *et al.*, 2024) and its response to climate. Neighbourhood species richness has been shown to
³⁶ influence individual functioning under various conditions (Fichtner *et al.*, 2018, 2020). However,
³⁷ this taxonomic diversity lens only offers limited insights into the mechanisms that drive the effects
³⁸ of neighbourhood diversity, and especially whether complementarity actually plays a major role
³⁹ in the mitigation of negative climate effects (Grossiord, 2020; Jucker *et al.*, 2014).

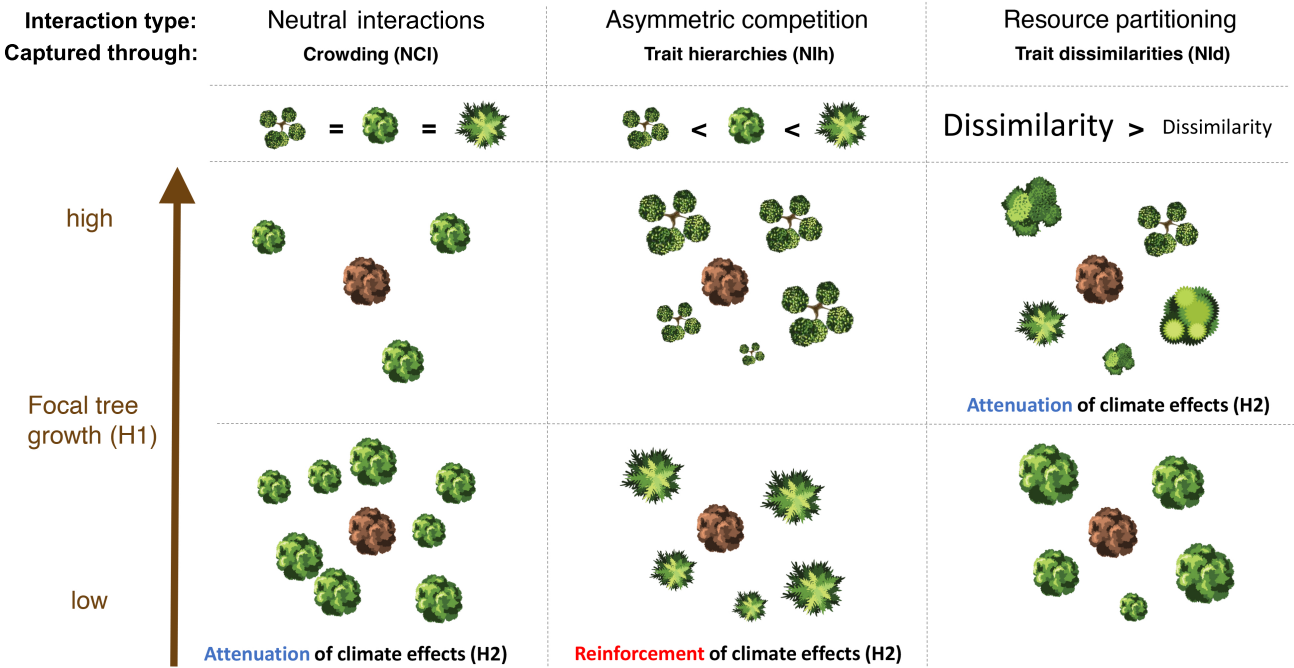


Figure 1. Conceptual illustration of different types of neighbourhood interactions, including neutral interactions, asymmetric competition and resource partitioning between a focal tree (brown) and its neighbouring trees (green). Neutral interactions can be captured by neighbourhood crowding indices (NCI), which depend solely on neighbourhood densities (i.e. the number, size and distance of neighbours). Asymmetric competition and resource partitioning can be respectively captured by the use of neighbourhood indices (NIh and NId) that include functional differences in the form of trait hierarchies (i.e. relative trait differences) or trait dissimilarities (i.e. absolute trait differences) between the focal tree and its neighbours. The expected effect of different types of neighbourhood interactions on individual tree growth (H1) and response to climate stress (H2), correspond to our hypotheses.

- 40 Neighbourhood effects on individual tree growth are the net outcome of simultaneous negative
 41 and positive interactions, which can be captured by different neighbourhood indices (Fig. 1) and
 42 whose relative importance may change when heat and drought stress occur (Grossiord, 2020).
 43 Negative neighbourhood effects can result from density dependent (i.e. neutral) interactions for
 44 shared resources (Jucker *et al.*, 2016; Pommerening & Sánchez Meador, 2018). While denser
 45 neighbourhoods can reinforce drought effects (Bottero *et al.*, 2017), for instance through increased
 46 consumption of water, they can simultaneously shelter trees from atmospheric climate extremes
 47 (Nemetschek *et al.*, 2024). Interactions may additionally be asymmetric, suggesting that differ-
 48 ences in functional strategies between tree species can result into competitive hierarchies between
 49 neighbours (Canham *et al.*, 2004; Pommerening & Sánchez Meador, 2018). Water spender neigh-

bours that exert strong pressure on the common water resource may have greater negative impacts on drought stress experienced by water conservative trees than conservative species have on them. Conversely, positive neighbourhood effects may result from facilitation (Brooker *et al.*, 2007) or greater functional dissimilarity indicating resource partitioning (Pommerening & Sánchez Meador, 2018), which could alleviate climate stress experienced by individual trees. Previous work on the relative contributions of different neighbourhood interactions on tree growth, captured by different indices, showed a key role of traits related to space, light and nutrients use (Fortunel *et al.*, 2016; Kunstler *et al.*, 2016; Uriarte *et al.*, 2010). As these traits offer little insights on water-use strategies and responses to water limitations (Maréchaux *et al.*, 2019; Wagner *et al.*, 2014), traits related to water relations may offer additional insight into neighbourhood interactions for water and elucidate their role in shaping individual response to droughts (Brodribb, 2017; Grossiord, 2020).

In a highly diverse Amazonian forest, we investigated how species differences in traits pertaining to plant-water relations and carbon use drive interactions between neighbouring trees and modulate individual growth response to heat and drought stress. We used hierarchical Bayesian models to evaluate the separate and interactive effects of i) climate variables indicating heat, atmospheric and soil water drought stress and ii) neighbourhood indices capturing the effects of neighbourhood crowding, trait hierarchies and dissimilarities on individual tree growth. Our analyses leveraged trait and 30-year long census data for 89 species from 15 permanent plots, some of which were subjected to initial selective logging and thinning, leading to contrasting neighbourhood structure, composition and dynamics. This long-term census data and its high temporal resolution (biennial) provides a broad range of neighbourhood and climatic conditions (Fig. S1) needed to study neighbourhood effects on climate responses of individual tree growth. We hypothesised that:

(H1) An individuals' growth is lower when surrounded by more neighbours (higher density), by superior competitors (stronger trait hierarchy) and more similar neighbours (lower trait dissimilarity) (Table 1).

(H2) Neighbourhood is more likely to buffer negative climate effects when trait dissimilarity is high or when being composed of more water conservative species. Conversely, high densities of

78 water-spender and dehydration tolerant species are more likely to accentuate negative drought-
79 related climate effects (Table 1).

80

81 Materials and Methods

82 Study site and inventory data

83 This study leverages 30 years of spatially-explicit inventory data from the CIRAD permanent
84 forest plots of the Paracou research station ($5^{\circ}18'N$, $52^{\circ}53'W$) in French Guiana. Paracou is a
85 tropical lowland forest site with an annual precipitation of 3102 mm yr^{-1} and a pronounced 3-
86 month dry season ($<100\text{ mm mo}^{-1}$) spanning from mid-August to mid-November, during which
87 wood production is reduced, and at the end of which water becomes limiting. Additionally a
88 shorter dry season can be observed in March (Aguilos *et al.*, 2019).

89 The plot network was established between 1984 and 1990 and consists of fifteen 6.25 ha forest
90 plots, covering 93.75 ha of predominantly terra-firme forest. In 1987, nine plots were subjected to
91 three intensities of silvicultural treatments including thinning, poison-girdling and selective logging.
92 These treatments resulted in 12–56% loss of above-ground biomass (Gourlet-Fleury *et al.*, 2004),
93 and led to contrasting community composition (Mirabel *et al.*, 2020) and neighbourhood densities
94 (Nemetschek *et al.*, 2024) between plots and years. Since then, tree inventories took place every two
95 years, during which the spatial location (precision 0.5 m), status (alive/dead) and circumference
96 (precision 0.5 cm, from which we calculated DBH), of each tree $\geq 10\text{ cm DBH}$ (diameter at breast
97 height, i.e. 1.3 m) was recorded (Derroire *et al.*, 2022b; Gourlet-Fleury *et al.*, 2004). More than 590
98 species and subspecies, from 227 genera and 63 families have been measured at the site (mean 142
99 species per hectare), with the dominant families being Fabaceae, Chrysobalanaceae, Lecythidaceae,
100 Sapotaceae and Burseraceae (Hérault *et al.*, 2011).

101 We calculated individual annualised absolute diameter growth rate (AGR, cm/yr) from DBH at
102 the end t and the start $t-2$ of 15 two-year census intervals between 1991 and 2021, excluding

103 aberrant and uncertain growth measurements (see Supplementary Methods S1 for details).

$$AGR_{i,s,t} = \frac{DBH_{i,s,t} - DBH_{i,s,t-2}}{2} \quad (\text{eqn 1})$$

104 Although most trees at Paracou were botanically identified, some individuals (<10%) only received
105 a vernacular name, mainly due to tree death before botanical identification could take place. To
106 infer the most likely association between the botanical and vernacular name for a given individual,
107 we used the vernabota R package ([Derroire et al. 2022a](#), see Supplementary Methods S2 for details).
108 While tree individuals with gapfilled species information were removed from the focal tree data,
109 they were kept in the neighbourhood data (see section Neighbourhood indices).

110 Climate data

111 To study the separate and interactive effects of climate and neighbours, we extracted mean monthly
112 averages of three climate variables from the high-resolution global TerraClimate data set ([Abat-](#)
113 [zoglou et al., 2018](#)): maximum temperature (Tmax), vapour pressure deficit (VPD) and climatic
114 water deficit (CWD), which have been shown to capture tropical tree responses to different aspects
115 of climate stress ([Bauman et al., 2022a](#); [Nemetschek et al., 2024](#)). Specifically, these climate indices
116 respectively capture heat stress, atmospheric evaporative demands and soil water availability, the
117 latter by relating precipitation to evapotranspiration. We expressed inter-annual variation in these
118 indices as the mean of monthly climate anomalies over each of the two-year census intervals, as fol-
119 lows (CA_t , Fig. S1): For each climate index and month, we calculated their deviations from their
120 respective 30-year monthly mean for the 1991-2021 period, before dividing them by their 30-year
121 monthly standard deviation. We then averaged these standardised monthly climate anomalies over
122 the 24 months prior to each census t ([Bauman et al. 2022a](#); [Nemetschek et al. 2024](#); [Rifai et al.](#)
123 [2018](#), see Methods S3). Doing so allowed us to directly interpret climate induced growth variations
124 as responses to higher climate stress than usual.

125 **Trait data**

126 To capture species water relations (Table 1), we measured leaf water potential at turgor loss point
127 (π_{tlp}), leaf minimum conductance (g_{min}) and leaf saturated water content (LSWC) in the dry
128 seasons of 2020 and 2021 (Nemetschek *et al.*, 2024). We selected target species according to their
129 abundance to maximise neighbourhood coverage for our growth models. In addition, we combined
130 our three water-related traits with data from previous field campaigns at Paracou (Levionnois *et al.*,
131 2021; Maréchaux *et al.*, 2015, 2019; Ziegler *et al.*, 2019). We further compiled data on bulk leaf
132 carbon isotope composition ($\delta^{13}\text{C}$), leaf area (LA), specific leaf area (SLA), leaf thickness (L_{thick}),
133 leaf toughness (L_{tough}) and wood specific gravity (WSG) from previous work conducted in French
134 Guiana (Baraloto *et al.*, 2010; Fortunel *et al.*, 2012; Vleminckx *et al.*, 2021). We subsequently
135 calculated species mean trait values from individual trait measurements. Our final trait dataset
136 includes complete trait information on 89 species (from 71 genera and 34 families), that together
137 represent 77% of all unique individual stems and 78% of growth measurements at Paracou. For
138 more information on the different traits and data sources see Table 1 and Nemetschek *et al.* (2024).

Table 1. Functional traits used in the study, and their functional significance. We additionally provide the sources from which data on each trait was compiled.

Organ	Trait	Abbreviation (Unit)	Function	Description	References	Data Source
Traits pertaining to plant water relations						
Leaf	Bulk leaf carbon stable isotope	$\delta^{13}\text{C}$ (‰)	Carbon-water use	High $\delta^{13}\text{C}$ translates into high intrinsic water-use efficiency (i.e. high photosynthetic rates relative to stomatal conductance) and therefore greater water conservation.	Farguhar et al. 1989, Cernusak et al. 2013, Scheidegger et al. 2000	Baraloto et al. 2010, Fortunel et al. 2012, Vlemminckx et al. 2021
Leaf	Water potential at turgor loss point	π_{tip} (MPa)	Drought tolerance or water conservation	Low π_{tip} translates into a greater ability to tolerate dehydration thereby maintaining stomatal conductance, hydraulic conductance and photosynthetic gas exchange at lower soil water potential. Conversely, high (i.e. less negative) π_{tip} indicates early stomatal closure during drought, which allows avoiding dehydration through water conservation.	Bartlett et al. 2012, Martin St-Paul et al. 2017	Marechaux et al. 2015, Marechaux et al. 2019, Nemetschek et al. 2024, Ziegler et al. 2019
Leaf	Minimum conductance	g_{min} (mmol m ⁻² s ⁻¹)	Water conservation	Low g_{min} translates into low residual water loss after stomatal closure through leaf cuticle and incompletely closed stomata, thereby avoiding dehydration through water conservation.	Blackman et al. 2019, Duursma et al. 2019, Machado et al. 2021	Levionnois et al. 2021, Nemetschek et al. 2024
Leaf	Leaf saturated water content	LSWC (%)	Water storage	High LSWC translates into leaf water reserves that may allow maintenance of leaf water potential when water supply becomes limited.	Blackman et al. 2019, Gleason et al. 2014, Luo et al. 2021	Nemetschek et al. 2024
Traits pertaining to carbon use						
Leaf	Leaf area	LA (cm ²)	Light capture	Large leaves intercept more light, have thick leaf boundary layer that limit heat exchange with surrounding air, but also higher transpiration rates.	Wright et al. 2017	Baraloto et al. 2010, Fortunel et al. 2012, Vlemminckx et al. 2021
Leaf	Specific leaf area	SLA (m ² kg ⁻¹)	Resource capture and defense	High SLA reflects greater allocation of dry mass to light interception than physical resistance and leaf lifespan and indicates aquisitive carbon-use strategy.	Osnas et al. 2013, Wright et al. 2004	Baraloto et al. 2010, Fortunel et al. 2012, Vlemminckx et al. 2021
Leaf	Leaf thickness	Lthick (mm)	Resource capture and defense	High Lthick reflects greater allocation of dry mass to structural support, physical resistance and leaf lifespan and indicates conservative carbon-use strategy.	Vile et al. 2005	Baraloto et al. 2010, Fortunel et al. 2012, Vlemminckx et al. 2021
Leaf	Leaf toughness	Ltough (N)	Resource capture and defense	High Ltough reflects greater allocation of dry mass to structural support, physical resistance and leaf lifespan and indicates conservative carbon-use strategy.	Kitajima and Poorter 2010	Baraloto et al. 2010, Fortunel et al. 2012, Vlemminckx et al. 2021
Wood	Stem wood specific gravity	WSG	Stem transport, structure and defense	High wood specific gravity reflects greater allocation of dry mass to mechanical strength and resistance to abiotic and biotic threats, and indicates conservative carbon-use strategy and slow growth.	Chave et al. 2009, Poorter et al. 2010,	Baraloto et al. 2010, Fortunel et al. 2012, Vlemminckx et al. 2021

¹³⁹ **Neighbourhood indices**

¹⁴⁰ For each individual focal tree i at the start of the growth census interval $t - 2$, we calculated three
¹⁴¹ neighbourhood indices within a radius of 10 m around the focal tree (Fortunel *et al.*, 2018; Lasky
¹⁴² *et al.*, 2014). To capture neighbourhood densities we calculated a neutral neighbourhood crowding
¹⁴³ index (NCI) as:

$$NCI_{i,t-2} = \sum_{\substack{j=1 \\ j \neq i}}^J \frac{DBH_{j,t-2}^2}{d_{i,j}} \quad (\text{eqn 2})$$

¹⁴⁴ where J is the number of neighbours within the 10-m radius and the influence of a given neighbour
¹⁴⁵ j on the focal tree i is proportional to its basal area (DBH_j^2) and declines linearly with its distance
¹⁴⁶ (d_{ij}) from the focal tree i .

¹⁴⁷ To respectively capture the effects of trait hierarchies and dissimilarities between the focal tree
¹⁴⁸ and its neighbours we calculated NIh and NId as the weighted average of trait hierarchies and
¹⁴⁹ dissimilarities between the focal tree and all its neighbours within the neighbourhood radius as:

$$NIh_{i,t-2} = \frac{1}{NCI_{i,t-2}} \times \left(\sum_{k=1}^K \lambda_{s,k} \sum_{\substack{j=1 \\ j \neq i}}^{J(k)} \frac{DBH_{j,t-2}^2}{d_{i,j}} \right) \quad (\text{eqn 3})$$

$$NId_{i,t-2} = \frac{1}{NCI_{i,t-2}} \times \left(\sum_{k=1}^K |\lambda_{s,k}| \sum_{\substack{j=1 \\ j \neq i}}^{J(k)} \frac{DBH_{j,t-2}^2}{d_{i,j}} \right) \quad (\text{eqn 4})$$

¹⁵⁰ where trait hierarchies are relative trait differences ($\lambda_{s,k} = trait_s - trait_k$) and trait dissimilarities
¹⁵¹ are absolute trait differences ($|\lambda_{s,k}| = |trait_s - trait_k|$) between the species s of focal tree i and
¹⁵² the species k of its $J(k)$ neighbours j . $\lambda_{s,k}$ increasingly differs from 0 with increasing relative
¹⁵³ (hierarchical) and absolute (dissimilarities) trait differences (Lasky *et al.*, 2014). The contribution
¹⁵⁴ of trait differences ($\lambda_{s,k}$) between the focal tree and each neighbour j to NIh and NId is weighted
¹⁵⁵ by the squared diameter of j and its inverse distance d_{ij} to the focal tree i (i.e. its contribution

to the *NCI*). For a given focal tree, *NIh* therefore increases when the focal tree has a relatively higher trait value in comparison to its neighbour and decreases when the focal tree has a relatively lower trait value in comparison to its neighbour. *NId* increases with increasing absolute trait differences (dissimilarities) between the focal and its neighbour, and these two indices are not influenced by the density of neighbours (see Table S3).

The 89 species for which complete information for all nine traits was available constitute our focal species. As *NIh* and *NId* require trait information for all neighbours within the neighbourhood, we gapfilled missing trait information for all remaining species using the year and plot specific community weighted mean. To reduce the influence of missing species trait information on neighbourhood effect estimates, we only selected focal trees for which at least 75% of their NCI belonged to species with available trait information. For more detailed information on neighbourhood indices and subsetting of focal individuals see Methods S4.

Models

We evaluated the separate and interactive effects of climate anomalies and neighbourhood indices (*NCI*, *NIh* and *NId*) on individual absolute growth rates (AGR) using hierarchical Bayesian models. To manage model complexity, we fitted models separately for each combination of (i) trait hierarchies (*NIh*) and dissimilarities (*NId*), (ii) the three climate variables (Tmax, VPD and CWD) and (iii) the nine functional traits, resulting in a total of 54 models. The model hierarchy consists of a community-level regression and a species-level response. The community-level regression models AGR responses to covariates via hyperparameters (i.e. statistical distributions from which species-level intercepts and slope coefficients arose), whereas the species-level captures species deviations from the community average parameters.

To reduce the influence of outliers and heteroscedasticity of the growth data, and to represent the multiplicative effects of covariates, we modelled the natural logarithm of absolute growth rates $\log(AGR)$ (Fortunel *et al.*, 2018; Héault *et al.*, 2011; Kunstler *et al.*, 2016). As we assumed tree growth to have a non-linear relationship with DBH (Canham *et al.*, 2004), *NCI* (Fortunel *et al.*,

182 2016), NIh and NId , we log-transformed DBH and all three neighbourhood indices prior to stan-
 183 dardisation (Fortunel *et al.*, 2018; Kunstler *et al.*, 2016). To allow for direct comparison of param-
 184 eter estimates within and between models and ease the assignment of plausible weakly-informative
 185 prior to the parameters (McElreath, 2020), $\log(AGR)$ and all covariates were standardised to mean
 186 zero and unit standard deviation, except for climate anomalies (Bauman *et al.*, 2022a; Nemetschek
 187 *et al.*, 2024). As our focal species cover a wide range of mean tree sizes, we standardised DBH to
 188 mean zero and unit standard deviation within species, to prevent confounding species differences
 189 in growth response to tree size with inter-specific variation in mean DBH (Fortunel *et al.*, 2018).
 190 For further details on variable transformation see Methods S5.

191 For each individual i of species s in plot p between censuses $t-2$ and t , we modelled the logarithm
 192 of tree growth with a normal distribution:

$$\log(AGR_{i,s,t,p}) \sim \mathcal{N}(\mu_{i,s,t,p}, \sigma^2) \quad (\text{eqn 5a})$$

193 where the mean $\mu_{i,s,t,p}$ is a linear function of tree size at the beginning of the census interval
 194 ($DBH_{i,t-2}$), monthly climate anomalies averaged over the census interval (CA_t), neutral neighbour-
 195 hood crowding index ($NCI_{i,t-2}$), one of the non-neutral neighbourhood index ($NI_{i,t-2}$) capturing
 196 either trait hierarchies ($NIh_{i,t-2}$) or trait dissimilarities ($NId_{i,t-2}$) at the beginning of the census
 197 interval, and their interactive effects with climate anomalies ($CA_t \times NCI_{i,t-2}$ and $CA_t \times NI_{i,t-2}$):

$$\begin{aligned}
 \mu_{i,s,t,p} = & \alpha_s + \beta_{1s} \times \log(DBH_{i,t-2}) + \beta_{2s} \times CA_t \\
 & + \beta_{3s} \times \log(NCI_{i,t-2}) + \beta_{4s} \times \log(NI_{i,t-2}) \\
 & + \beta_{5s} \times CA_t \times \log(NCI_{i,t-2}) + \beta_{6s} \times CA_t \times \log(NI_{i,t-2}) \\
 & + \gamma_p + \epsilon_i
 \end{aligned} \quad (\text{eqn 5b})$$

198 α_s and β_{1-6s} are species-specific coefficients representing intrinsic AGR (α_s), and species responses

199 to tree size (β_{1s}), climate anomalies (β_{2s}), neighbourhood crowding (β_{3s}), hierarchical or dissimilarity
 200 neighbourhood index (β_{4s}) as well as interactive effect of climate anomalies with neighbourhood
 201 crowding index (β_{5s}), or with hierarchical or dissimilarity neighbourhood index (β_{6s}). We further
 202 allowed intercepts to vary by plots γ_p and individuals ϵ_i , to capture part of the unexplained growth
 203 variation related to plots and individuals (Bauman *et al.*, 2022a; Fortunel *et al.*, 2018).

204 Species intrinsic AGR α_s and AGR response to covariates β_{1-6s} for the s species were modelled
 205 using a multivariate normal distribution:

$$\begin{pmatrix} \alpha_s \\ \beta_{1s} \\ \vdots \\ \beta_{6s} \end{pmatrix} \sim MVNormal \left[\begin{pmatrix} \alpha \\ \beta_1 \\ \vdots \\ \beta_6 \end{pmatrix}, S \right] \quad (\text{eqn 5c})$$

206 where α represents the community level intrinsic growth rate, β_{1-6} the overall effect of covariates
 207 on AGR across all species and S is a covariance matrix. Modelling all species-level parameters as a
 208 multivariate normal distribution allows sharing information across species, thus improving the fit
 209 for poorly represented species, while preventing overfitting (McElreath, 2020). For the full model
 210 equation and the specified weakly informative priors see Methods S6.

211 Models were fitted in the R environment (R Core Team, 2021; RStudio Team, 2020) on the
 212 Meso@LR HPC cluster using the package brms (Bürkner, 2017). Bayesian updating of param-
 213 eters was performed via the No-U-Turn Sampler (NUTS) in Stan (Carpenter *et al.*, 2017) using
 214 CmdStanR (Stan Development Team, 2022). We used four chains and 3000 iterations (1500 warm
 215 up) per chain. Chains of all models mixed well and generally converged within 1500 iterations
 216 (Rhat between 1 and 1.05). Model parameter posteriors were summarised through their median
 217 and 90% highest posterior density interval (HPDI) using the packages tidyverse (Wickham *et al.*,
 218 2019) and tidybayes (Kay, 2022). To assess the model goodness of fit, we calculated conditional
 219 and marginal R^2 , which represent respectively the fraction of variance explained by the fixed and
 220 random terms and by the fixed terms only, using the bayes_R2() function of the brms package

221 (Bürkner, 2017). The function calculates a Bayesian version of R^2 for regression models (Gelman
222 et al., 2019). Our models had high a explanatory power, with a mean conditional R^2 of 61% and
223 showed to be stable across climate-trait model combinations. For detailed information on condi-
224 tional and marginal R^2 values for each model fit see Table S1 and for model stability see Methods
225 S7.

226 Results

227 Tree growth response to neighbourhood indices

228 Individual tree growth strongly declined (negative β_3) with increasing NCI , while effect sizes were
229 smaller for both NIh and NId (Fig. 2). Greater NIh can both increase (positive β_4) or reduce
230 (negative β_4) tree growth, while increasing NId consistently increased (positive β_4) tree growth.
231 More specifically, higher NIh in $\delta^{13}\text{C}$ and SLA increased growth, indicating that focal trees grew
232 faster when their intrinsic water-use efficiency and specific leaf area was higher than those of their
233 neighbours. On the other hand, growth declined with increasing NIh in π_{tlp} , g_{\min} , LA, L_{thick} ,
234 L_{though} or WSG, indicating that focal trees grew slower when they had higher water potential at
235 turgor loss point, higher minimum conductance, larger, thicker or tougher leaves as well as higher
236 wood specific gravity than that of their neighbours. Lastly, higher NId in $\delta^{13}\text{C}$, π_{tlp} , LSWC, g_{\min} ,
237 LA, SLA, L_{thick} and WSG positively influenced tree growth, indicating trees grew faster when their
238 neighbours were more dissimilar in these trait values.

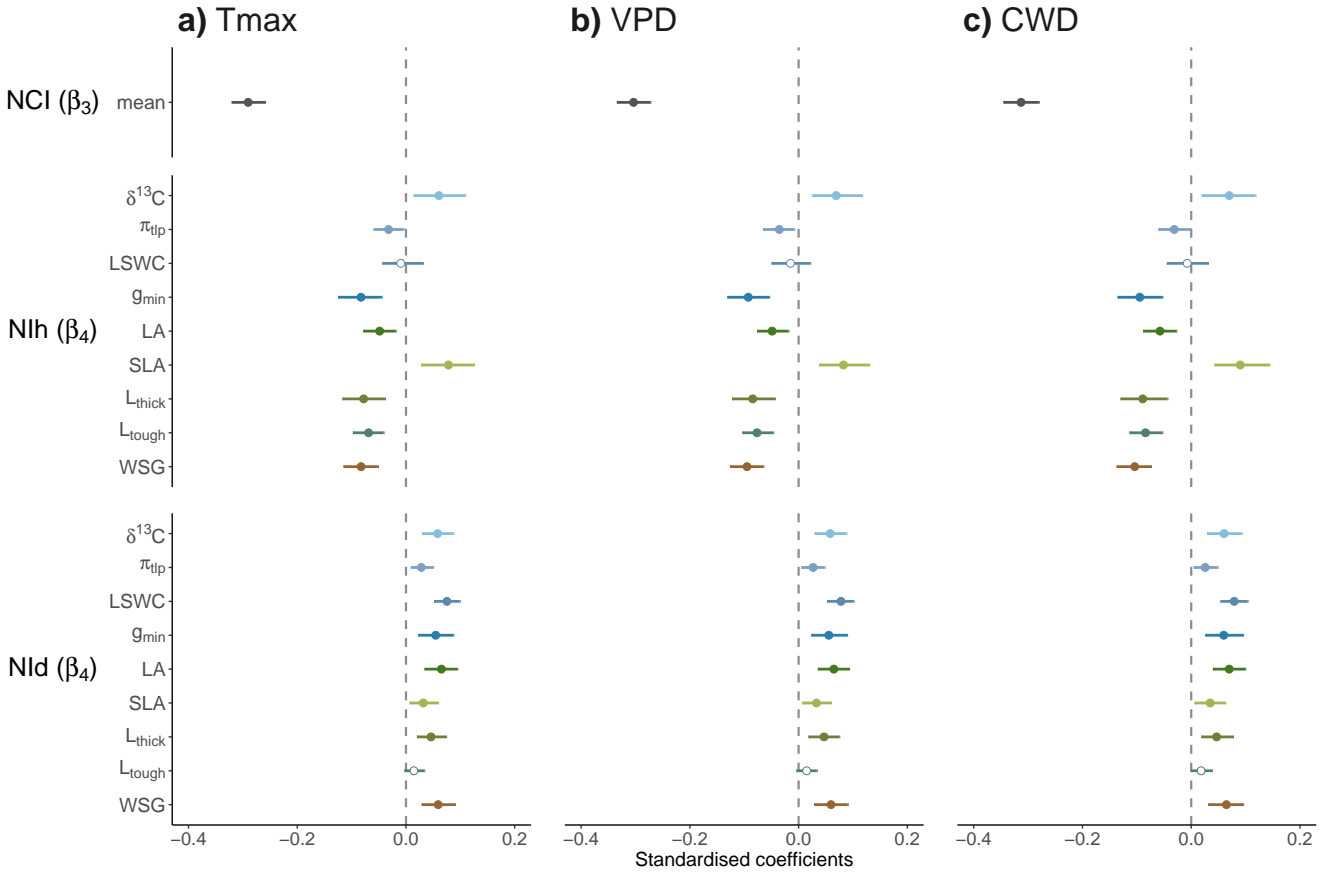


Figure 2. Community-level effect of neutral neighbourhood crowding (NCI, β_3), hierarchical (NIh, β_4) and dissimilarity (NId, β_4) neighbourhood index on tree growth. Standardised coefficients from a) Tmax, b) VPD and c) CWD models are shown for NCI as mean estimates across the two NI and nine trait models (see Fig. S2 and S3 for separate estimates) and for NIh and NId separately for each of the nine trait models: carbon ($\delta^{13}\text{C}$) isotope composition, water potential at turgor loss point (π_{tlp}), leaf saturated water content (LSWC), minimum conductance (g_{\min}), leaf area (LA), specific leaf area (SLA), leaf thickness (L_{thick}), leaf toughness (L_{tough}) and wood specific gravity (WSG). Circles show posterior medians of standardised coefficients, and lines indicate 90% HPDIs. Model covariates were considered to have a clear effect when the slope coefficients 90%-HPDIs did not encompass zero. Filled circles indicate clear negative and positive effects (i.e. slope coefficient 90% HPDI not encompassing zero) and empty circles indicate no clear effects. Positive β_{3-4} values indicate faster growth with increasing neighbourhood index, while negative β_{3-4} values indicate slower growth with increasing neighbourhood index (details in Table S2).

239 **Tree growth response to interactive effects of climate anomalies and
240 neighbourhood indices**

241 Positive anomalies in maximum temperature (Tmax), vapour pressure deficit (VPD) and climatic
242 water deficit (CWD) reduced tree growth (negative β_2). Moreover, higher NCI led to a clear
243 buffering (positive β_5 , Fig. 3) of negative effects of Tmax, while also showing a strong trend to

244 buffer negative effects of VPD and CWD. Only a few trait differences between the focal tree and its
245 neighbours led to a clear modulation of growth through trait hierarchies (NIh) or dissimilarities
246 (NId), and these effects depended on the climate variable. More specifically, negative effects
247 of Tmax were reinforced (negative β_6) for trees with relatively higher $\delta^{13}\text{C}$ (higher NIh) than
248 their neighbours and buffered (positive β_6) for trees with relatively higher π_{tlp} and g_{\min} than their
249 neighbourhood (higher NIh). Furthermore, negative effects of Tmax were reinforced (negative β_6)
250 with increasing trait dissimilarities (higher NId) in LSWC but attenuated (positive β_6) for trees
251 surrounded by more dissimilar neighbours regarding $\delta^{13}\text{C}$, L_{thick} and L_{though} . While increasing
252 trait hierarchies in LA, L_{thick} and L_{though} reinforced the negative effects of VPD on tree growth
253 (negative β_6), increasing trait hierarchies in π_{tlp} and greater dissimilarity (higher NId) in L_{though}
254 led to significant buffering (positive β_6). Lastly, focal trees suffered lower growth declines (positive
255 β_6) from higher CWD when having relatively higher LA than their neighbours (higher NIh) or
256 having more dissimilar neighbours regarding π_{tlp} (higher NId). However, greater dissimilarities in
257 $\delta^{13}\text{C}$ (higher NId) accentuated negative effects of CWD (negative β_6).

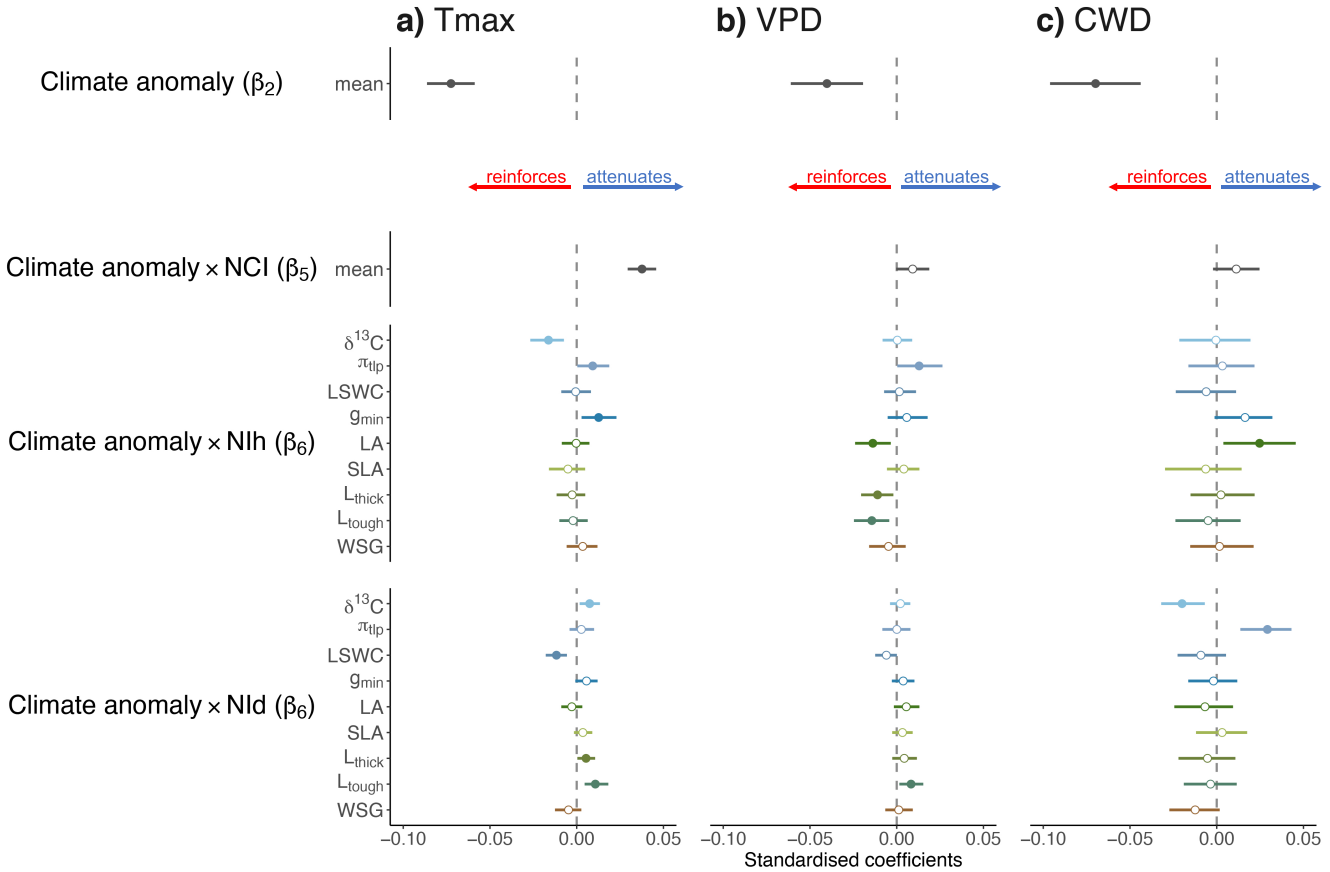


Figure 3. Community-level effects of climate anomaly (β_2), and the interactions between climate anomaly and neutral neighbourhood crowding (Climate anomaly \times NCI, β_5), hierarchical (Climate anomaly \times NIH, β_6) and dissimilarity (Climate anomaly \times NId, β_6) neighbourhood index on tree growth. Standardised coefficients from a) Tmax, b) VPD and c) CWD models are shown for climate anomalies and its interaction with NCI as mean estimates across the two NI and nine trait models (see Fig. S2 and S3 for separate estimates) and for the interaction between climate anomaly and NIH and NId separately for each of the nine trait models: carbon ($\delta^{13}\text{C}$) isotope composition, water potential at turgor loss point (π_{tlp}), leaf saturated water content (LSWC), minimum conductance (g_{\min}), leaf area (LA), specific leaf area (SLA), leaf thickness (L_{thick}), leaf toughness (L_{tough}) and wood specific gravity (WSG). Circles show posterior medians of standardised coefficients, and lines indicate 90% HPDIs. Model covariates were considered to have a clear effect when the slope coefficients 90%-HPDIs did not encompass zero. Filled circles indicate clear negative and positive effects (i.e. slope coefficient 90%-HPDI not encompassing zero) and empty circles indicate no clear effects. Positive β_{5-6} values indicate a buffering effect of either NCI or NI, while negative β_{5-6} values indicate an accentuating effect of either NCI or NI (details in Table S2).

258 Discussion

259 Using 30 years of high temporal resolution census data in a highly diverse tropical forest, we studied
 260 how the neighbourhood context influences tree growth in 89 tree species and its responses to heat as
 261 well as atmospheric and soil water drought stress. Our results reveal that neutral and asymmetric

competition act in concert with resource partitioning to shape tropical tree growth (Fig. 1 and 2). We further show that the local neighbourhood context can both attenuate or reinforce the negative effects of heat (Tmax), atmospheric (VPD) and soil water drought (CWD) stress (Fig. 2, see Nemetschek *et al.* 2024 for detailed discussion on effects of climate anomalies). Our analyses integrate for the first time trait differences of a broad suite of functional traits pertaining to plant water-relations and carbon-use (Table 1). This provides novel insights on the potential mechanisms that underlie negative and positive neighbourhood interactions mediated by trait differences both in normal and anomalous climate years.

Neighbourhood crowding (*NCI*), capturing neighbourhood density, strongly reduced individual tree growth (Fig. 1) and had by far the largest effect size of any of the six tested model covariates. This suggests that competition for shared space and resources is a key driver of tree growth at Paracou (Nemetschek *et al.*, 2024), and that competitive interactions between neighbouring trees are foremost driven by their size and proximity in space (Laurans *et al.*, 2014; Moravie *et al.*, 1997). Previous studies have shown that neighbourhood taxonomic diversity can positively influence tree performance, likely through increased functional dissimilarity between neighbours promoting resource partitioning (Ammer, 2019; Forrester & Bauhus, 2016). Our results provide direct and strong support of this hypothesis as greater dissimilarity in all nine tested traits consistently stimulated individual tree growth at our site (Fig. 2). Greater dissimilarity between neighbours in traits related to carbon use and root strategies have also previously been shown to increase tropical and subtropical tree performance (Fortunel *et al.*, 2016; Huang *et al.*, 2022; Lasky *et al.*, 2014; Uriarte *et al.*, 2010). Here we show for the first time that this extends to traits pertaining to leaf water relations ($\delta^{13}\text{C}$, π_{tlp} , LSWC, g_{\min}), uncovering the importance of complementary water-use and drought response strategies even in predominantly light- rather than water-limited tropical forests such as Paracou (Wagner *et al.*, 2016). This complementarity may be especially beneficial when a shift from light- to water-limitation can be observed (Meng *et al.*, 2022).

Providing further evidence for the importance of interactions for water at the neighbourhood scale, we show that greater trait hierarchies, which capture asymmetric neighbourhood interactions (Fig. 1), in water-related traits significantly influence tree growth (Fig. 2). Our results suggest that

a higher water use efficiency (higher $\delta^{13}\text{C}$), a greater ability to maintain physiological functioning under decreasing water availability (more negative π_{tlp}) and conserve water under drought stress (lower g_{\min}) than its neighbours may provide a competitive advantage, as reflected by faster growth. Contrasting to our findings for water-related traits and previous research (Fortunel *et al.*, 2016; Kunstler *et al.*, 2016), greater conservatism in carbon use relative to neighbours (lower SLA and greater L_{thick} , L_{tough} and WSG) was consistently associated to reduced tree growth. This highlights that greater resource conservatism in comparison to neighbours does not always result in a competitive advantage in tropical forests. Having more conservative carbon-use strategies than one's neighbours implies being surrounded by more resource acquisitive neighbours that may faster deplete common resources (Garbowski *et al.*, 2020; Goldberg, 1990). Specifically, faster growth at the expense of less mechanically resistant leaf and wood tissue (Chave *et al.*, 2009; Reich, 2014) promotes fast colonisation of forest gaps both vertically and horizontally (Westoby *et al.*, 2002), which constitutes a strong competitive advantage in disturbed plots making up 51% of growth observations at Paracou.

Beside its importance in shaping tree growth in normal years, our results clearly show that the neighbourhood context has the potential to modulate individual growth responses to climate stress (Fig. 3). In line with our previous study (Nemetschek *et al.*, 2024), we found that denser neighbourhoods consistently attenuate negative climate effects on tree growth. Denser neighbourhoods can physically shelter trees from extreme atmospheric climate stress, thereby improving local microclimatic conditions (De Frenne *et al.*, 2019; Tymen *et al.*, 2017; Wright, 2024). Simultaneously, neighbourhood taxonomic diversity can influence growth responses to drought (Grossiord, 2020). If resource partitioning is a key driver of positive diversity effects on drought resistance, their magnitude should depend on the functional identity of focal trees (Fichtner *et al.*, 2020), that of their neighbours and ultimately on their functional differences. Here we showed that greater trait dissimilarities can indeed increase individual growth resistance to climate stress. However, this effect can differ across traits and climate variables. Greater dissimilarities in leaf economics traits tended to buffer negative effects of the atmospheric climate variables Tmax (for L_{thick} and L_{tough}) and VPD (for L_{thick}). Increased complementarity in leaf morphology can indicate greater canopy

space filling (Forrester & Bauhus 2016, but see Hildebrand *et al.* 2021), which likely increases thermal insulation (De Frenne *et al.*, 2019; Zhang *et al.*, 2022). Conversely, greater dissimilarities in π_{tlp} mitigated negative effects of soil water stress (CWD). π_{tlp} is a key drought tolerance trait (Bartlett *et al.*, 2012) and a strong predictor of leaf water potential at stomatal closure (Martin-StPaul *et al.*, 2017; Rodriguez-Dominguez *et al.*, 2016). In line with our findings, complementarity in stomatal regulation and drought response strategies have previously been suggested to reduce plant water stress via its positive effect on local soil moisture status (Grossiord, 2020; Moreno *et al.*, 2023). In contrast to our expectations, we showed that greater trait dissimilarities also hold the potential to reinforce climate stress depending on the climatic stressors. For instance, complementarity in water-use efficiency ($\delta^{13}\text{C}$), which increased tree growth in normal years, attenuated negative effects of heat stress (Tmax), but reinforced negative effects of soil water stress (CWD). This suggests that rather than greater dissimilarity in certain traits capturing water-use strategies, greater overall water conservation at the neighbourhood scale may be beneficial under water limited conditions.

In line with this assumption, our results indicate that the competitive advantage of water-conservative species observed in normal years decreases in extreme climate years, as the negative effect of a higher consumption of water by the neighbourhood becomes more important (Fig. 2 and 3). For instance, greater water use efficiency (higher $\delta^{13}\text{C}$) relative to neighbours benefited individual tree growth in normal years, but reinforced negative effects of temperature stress (Tmax). Higher temperatures can lead to increased evapotranspiration, hence greater abundances of relatively less water conservative neighbours likely exert greater pressure on local soil water resources when temperature stress occurs (Grossiord *et al.*, 2014; Mas *et al.*, 2024). Conversely, greater water spenders relative to their neighbours tended to be more buffered: trees with higher residual water loss (g_{\min}) or larger LA relative to their neighbours grew slower in normal years but suffered less from negative effects of either temperature (Tmax) or soil water (CWD) stress. Larger leaves require more cooling through (higher) transpiration rates, which necessitates greater water supply per unit leaf area (Wright *et al.*, 2017). Our results therefore provide strong evidence for the positive effect of water conservative species on local soil water availability during drought and heat waves, which

346 may particularly benefit water spender species ([Mas *et al.*, 2024](#); [Moreno *et al.*, 2023](#)). These find-
347 ings can also provide mechanistic insights to why species with low drought tolerance profit most
348 from neighbourhood diversity during drought, as shown by [Fichtner *et al.* 2020](#). Conversely our
349 results indicate that water spender tree neighbours decrease water resources to the detriment of
350 the focal tree ([Garbowski *et al.*, 2020](#); [Goldberg, 1990](#)), increasing the climate stress experienced
351 particularly for water conservative species.

352 As forest ecosystems are increasingly likely to experience environmental conditions beyond their
353 normal range, understanding if currently observed biotic interactions will hold in a changing climate
354 is crucial ([Grossiord *et al.*, 2019](#)). By considering neighbourhood differences in water-related traits
355 in addition to carbon-related ones, our study shows that the consistent positive effect of resource
356 partitioning observed under normal conditions becomes more complex in climatically stressful
357 years. Similarly, trees profit from greater conservatism in water use in normal years, but as climate
358 stress increases, become increasingly affected by their neighbours' overall water consumption. Our
359 findings suggest that climate-change adapted forest management should carefully consider species'
360 water-use strategies and their interactions ([Forrester *et al.*, 2016](#)). We also stress the importance of
361 moving beyond the taxonomic diversity lens to understand how different types of neighbourhood
362 interactions affect tree performance in these new conditions. This provides a promising way forward
363 to assess the productivity and resilience of entire forest ecosystems under climate change.

³⁶⁴ **Acknowledgements**

We thank the many colleagues who participated in field and lab work for trait data collection in French Guiana and at the University of Vienna, especially Coralie Dalban-Pilon, Jocelyn Cazal, Stéphane Fourtier, Jean-Yves Goret, Paul Mischler, Gaëlle Jaouen, Laetitia Proux, Camille Giard Tercieux, Jeanne Clément, Ghislain Vieilledent and Sylvain Schmitt. We thank the CIRAD fieldwork team for the tree inventory, and Pascal Petronelli, Giacomo Sellan and Julien Engel for botanical identification. We thank Charlotte Grossiord, Raphaël Pélissier and Stefan Dullinger for helpful discussions. The modelling work has been realised with the support of Meso@LR-Platform at the University of Montpellier. We thank the Meso@LR team, in particular Bertrand Pitollat, and Philippe Verley for technical support. DN was supported by a PhD grant co-funded by Cirad and ‘Centre d’Etude de la Biodiversité Amazonienne’, an ‘Investissements d’Avenir’ grant managed by Agence Nationale de la Recherche (CEBA, ref. ANR-10-LABX- 25-01). This work has benefited from a grant (ManagForRes project) from Office Français de la Biodiversité (OFB) and ‘Centre Méditerranéen de l’Environnement et de la Biodiversité’, an ‘Investissements d’Avenir’ grant managed by Agence Nationale de la Recherche (CeMEB, ref. ANR-10-LABX-04-01). This work was also supported by the Institut de Recherche pour le Développement (IRD).

380 **List of Supporting Information**

381 In file SupportingInformation_1.pdf

382 **Figure S1.** Adapted figure from Nemetschek et al. (2024): Mean standardised climate anomalies
383 at Paracou for the two-year census intervals over the study period.

384 **Figure S2.** Standardised regression coefficients of community level parameter estimates from NIH
385 models.

386 **Figure S3.** Standardised regression coefficients of community level parameter estimates from NID
387 models.

388 **Methods S1.** Corrections of tree inventory data.

389 **Methods S2.** Gapfilling of missing species information.

390 **Methods S3.** Calculation of climate anomalies.

391 **Methods S4.** Additional information on neighbourhood indices.

392 **Methods S5.** Transformation of response variable and model covariates.

393 **Methods S6.** Full model equation.

394 **Methods S7.** Information on model stability.

395

396 In file SupportingInformation_2.xlsx

397 **Table S1.** Conditional and marginal R² estimates models.

398 **Table S2.** Standardised regression coefficients of community level parameters and group-level
399 sigmas.

400 **Table S3.** Pairwise Pearson correlation coefficients between neighbourhood indices.

401

References

- Abatzoglou, J.T., Dobrowski, S.Z., Parks, S.A. & Hegewisch, K.C. (2018). TerraClimate, a highresolution global dataset of monthly climate and climatic water balance from 1958–2015. *Scientific Data*, 5, 170191.
- Aguilos, M., Stahl, C., Burban, B., Hérault, B., Courtois, E., Coste, S., et al. (2019). Interannual and Seasonal Variations in Ecosystem Transpiration and Water Use Efficiency in a Tropical Rainforest. *Forests*, 10, 14.
- Allen, C.D., Macalady, A.K., Chenchouni, H., Bachelet, D., McDowell, N., Vennetier, M., et al. (2010). A global overview of drought and heat-induced tree mortality reveals emerging climate change risks for forests. *Forest Ecology and Management*, 259, 660–684.
- Ammer, C. (2019). Diversity and forest productivity in a changing climate. *New Phytologist*, 221, 50–66.
- Anderegg, W.R.L., Konings, A.G., Trugman, A.T., Yu, K., Bowling, D.R., Gabbitas, R., et al. (2018). Hydraulic diversity of forests regulates ecosystem resilience during drought. *Nature*, 561, 538–541.
- Baraloto, C., Timothy Paine, C.E., Poorter, L., Beauchene, J., Bonal, D., Domenach, A.M., et al. (2010). Decoupled leaf and stem economics in rain forest trees. *Ecology Letters*, 13, 1338–1347.
- Bartlett, M.K., Scoffoni, C. & Sack, L. (2012). The determinants of leaf turgor loss point and prediction of drought tolerance of species and biomes: a global meta-analysis. *Ecology Letters*, 15, 393–405.
- Bauman, D., Fortunel, C., Cernusak, L.A., Bentley, L.P., McMahon, S.M., Rifai, S.W., et al. (2022a). Tropical tree growth sensitivity to climate is driven by species intrinsic growth rate and leaf traits. *Global Change Biology*, 28, 1414–1432.
- Bauman, D., Fortunel, C., Delhaye, G., Malhi, Y., Cernusak, L.A., Bentley, L.P., et al. (2022b). Tropical tree mortality has increased with rising atmospheric water stress. *Nature*, 608, 528–533.

Belote, R.T., Prisley, S., Jones, R.H., Fitzpatrick, M. & de Beurs, K. (2011). Forest productivity and tree diversity relationships depend on ecological context within mid-Atlantic and Appalachian forests (USA). *Forest Ecology and Management*, 261, 1315–1324.

Blackman, C.J., Creek, D., Maier, C., Aspinwall, M.J., Drake, J.E., Pfautsch, S., *et al.* (2019). Drought response strategies and hydraulic traits contribute to mechanistic understanding of plant dry-down to hydraulic failure. *Tree Physiology*, 39, 910–924.

Bottero, A., D'Amato, A.W., Palik, B.J., Bradford, J.B., Fraver, S., Battaglia, M.A. & Asherin, L.A. (2017). Density-dependent vulnerability of forest ecosystems to drought. *Journal of Applied Ecology*, 54, 1605–1614.

Brodribb, T.J. (2017). Progressing from ‘functional’ to mechanistic traits. *New Phytologist*, 215, 9–11.

Brooker, R.W., Maestre, F.T., Callaway, R.M., Lortie, C.L., Cavieres, L.A., Kunstler, G., *et al.* (2007). Facilitation in plant communities: the past, the present, and the future. *Journal of Ecology*, 96, 18–34.

Bürkner, P.C. (2017). brms: An R Package for Bayesian Multilevel Models Using Stan. *Journal of Statistical Software*, 80, 1–28.

Canham, C.D., LePage, P.T. & Coates, K.D. (2004). A neighborhood analysis of canopy tree competition: effects of shading versus crowding. *Canadian Journal of Forest Research*, 34, 778–787.

Carpenter, B., Gelman, A., Hoffman, M.D., Lee, D., Goodrich, B., Betancourt, M., *et al.* (2017). Stan: A Probabilistic Programming Language. *Journal of Statistical Software*, 76, 1–32.

Cernusak, L.A., Ubierna, N., Winter, K., Holtum, J.A.M., Marshall, J.D. & Farquhar, G.D. (2013). Environmental and physiological determinants of carbon isotope discrimination in terrestrial plants. *New Phytologist*, 200, 950–965.

Chave, J., Coomes, D., Jansen, S., Lewis, S.L., Swenson, N.G. & Zanne, A.E. (2009). Towards a worldwide wood economics spectrum. *Ecology Letters*, 12, 351–366.

Crawford, M.S., Barry, K.E., Clark, A.T., Farrior, C.E., Hines, J., Ladouceur, E., *et al.* (2021). The function-dominance correlation drives the direction and strength of biodiversity–ecosystem functioning relationships. *Ecology Letters*, 24, 1762–1775.

De Frenne, P., Zellweger, F., Rodríguez-Sánchez, F., Scheffers, B.R., Hylander, K., Luoto, M., *et al.* (2019). Global buffering of temperatures under forest canopies. *Nature Ecology & Evolution*, 3, 744–749.

Derroire, G., Aubry-Kientz, M., Mirabel, A., Marcon, E. & Bruno, H. (2022a). vernabota: Association between vernacular and botanical names for Guyafor data.

Derroire, G., Hérault, B., Rossi, V., Blanc, L., Gourlet-Fleury, S. & Schmitt, L. (2022b). Data from: *Paracou plot data*. CIRAD Dataverse. Available at: <https://doi.org/10.18167/DVN1/NSCWF0>, <https://doi.org/10.18167/DVN1/Q8V2YI>, <https://doi.org/10.18167/DVN1/LIVCEK>, <https://doi.org/10.18167/DVN1/HWTD4U>, <https://doi.org/10.18167/DVN1/HIGNWQ>.

Duursma, R.A., Blackman, C.J., Lopéz, R., Martin-StPaul, N.K., Cochard, H. & Medlyn, B.E. (2019). On the minimum leaf conductance: its role in models of plant water use, and ecological and environmental controls. *New Phytologist*, 221, 693–705.

Farquhar, G.D., Ehleringer, J.R. & Hubick, K.T. (1989). Carbon Isotope Discrimination and Photosynthesis. *Annual Review of Plant Physiology and Plant Molecular Biology*, 40, 503–537.

Fichtner, A., Härdtle, W., Bruelheide, H., Kunz, M., Li, Y. & Von Oheimb, G. (2018). Neighbourhood interactions drive overyielding in mixed-species tree communities. *Nature Communications* 2018 9:1, 9, 1–8.

Fichtner, A., Schnabel, F., Bruelheide, H., Kunz, M., Mausolf, K., Schuldt, A., *et al.* (2020). Neighbourhood diversity mitigates drought impacts on tree growth. *Journal of Ecology*, 108, 865–875.

Forrester, D.I. & Bauhus, J. (2016). A Review of Processes Behind Diversity—Productivity Relationships in Forests. *Current Forestry Reports*, 2, 45–61.

Forrester, D.I., Bonal, D., Dawud, S., Gessler, A., Granier, A., Pollastrini, M. & Grossiord, C. (2016). Drought responses by individual tree species are not often correlated with tree species diversity in European forests. *Journal of Applied Ecology*, 53, 1725–1734.

Fortunel, C., Fine, P.V.A. & Baraloto, C. (2012). Leaf, stem and root tissue strategies across 758 Neotropical tree species. *Functional Ecology*, 26, 1153–1161.

Fortunel, C., Lasky, J.R., Uriarte, M., Valencia, R., Wright, S.J., Garwood, N.C. & Kraft, N. (2018). Topography and neighborhood crowding can interact to shape species growth and distribution in a diverse Amazonian forest. *Ecology*, 99, 2272–2283.

Fortunel, C., Valencia, R., Wright, S.J., Garwood, N.C. & Kraft, N.J. (2016). Functional trait differences influence neighbourhood interactions in a hyperdiverse Amazonian forest. *Ecology letters*, 19, 1062–1070.

Garbowski, M., Avera, B., Bertram, J.H., Courkamp, J.S., Gray, J., Hein, K.M., et al. (2020). Getting to the root of restoration: considering root traits for improved restoration outcomes under drought and competition. *Restoration Ecology*, 28, 1384–1395.

Gelman, A., Goodrich, B., Gabry, J. & Vehtari, A. (2019). R-squared for Bayesian Regression Models. *The American Statistician*, 73, 307–309.

Gleason, S.M., Blackman, C.J., Cook, A.M., Laws, C.A. & Westoby, M. (2014). Whole-plant capacitance, embolism resistance and slow transpiration rates all contribute to longer desiccation times in woody angiosperms from arid and wet habitats. *Tree Physiology*, 34, 275–284.

Goldberg, D.E. (1990). Components of Resource Competition in Plant Communities. In: *Perspectives on Plant Competition* (eds. Grace, J.B. & Tilman, D.). Academic Press, Cambridge, pp. 27–49.

Gourlet-Fleury, S., Guehl, J.M. & Laroussinie, O.E. (2004). *Ecology and management of a neotropical rainforest: lessons drawn from Paracou, a long-term experimental research site in French Guiana*. Elsevier, Paris.

Grossiord, C. (2020). Having the right neighbors: how tree species diversity modulates drought impacts on forests. *New Phytologist*, 228, 42–49.

Grossiord, C., Gessler, A., Granier, A., Pollastrini, M., Bussotti, F. & Bonal, D. (2014). Interspecific competition influences the response of oak transpiration to increasing drought stress in a mixed Mediterranean forest. *Forest Ecology and Management*, 318, 54–61.

Grossiord, C., Sevanto, S., Bonal, D., Borrego, I., Dawson, T.E., Ryan, M., *et al.* (2019). Prolonged warming and drought modify belowground interactions for water among coexisting plants. *Tree Physiology*, 39, 55–63.

Héault, B., Bachelot, B., Poorter, L., Rossi, V., Bongers, F., Chave, J., *et al.* (2011). Functional traits shape ontogenetic growth trajectories of rain forest tree species. *Journal of Ecology*, 99, 1431–1440.

Higgins, S.I., Conradi, T. & Muhoko, E. (2023). Shifts in vegetation activity of terrestrial ecosystems attributable to climate trends. *Nature Geoscience*, 16, 147–153.

Hildebrand, M., Perles-Garcia, M.D., Kunz, M., Härdtle, W., von Oheimb, G. & Fichtner, A. (2021). Tree-tree interactions and crown complementarity: The role of functional diversity and branch traits for canopy packing. *Basic and Applied Ecology*, 50, 217–227.

Huang, Z., Ran, S., Fu, Y., Wan, X., Song, X., Chen, Y. & Yu, Z. (2022). Functionally dissimilar neighbours increase tree water use efficiency through enhancement of leaf phosphorus concentration. *Journal of Ecology*, 110, 2179–2189.

Jucker, T., Bouriaud, O., Avacaritei, D., Dănilă, I., Duduman, G., Valladares, F. & Coomes, D.A. (2014). Competition for light and water play contrasting roles in driving diversity–productivity relationships in Iberian forests. *Journal of Ecology*, 102, 1202–1213.

Jucker, T., Sanchez, A.C., Lindsell, J.A., Allen, H.D., Amable, G.S. & Coomes, D.A. (2016). Drivers of aboveground wood production in a lowland tropical forest of West Africa: teasing apart the roles of

tree density, tree diversity, soil phosphorus, and historical logging. *Ecology and Evolution*, 6, 4004–4017.

Kay, M. (2022). tidybayes: Tidy Data and Geoms for Bayesian Models.

Kitajima, K. & Poorter, L. (2010). Tissue-level leaf toughness, but not lamina thickness, predicts sapling leaf lifespan and shade tolerance of tropical tree species. *New Phytologist*, 186, 708–721.

Kunstler, G., Falster, D., Coomes, D.A., Hui, F., Kooymann, R.M., Laughlin, D.C., *et al.* (2016). Plant functional traits have globally consistent effects on competition. *Nature*, 529, 204–207.

Lasky, J.R., Uriarte, M., Boukili, V.K. & Chazdon, R.L. (2014). Trait-mediated assembly processes predict successional changes in community diversity of tropical forests. *Proceedings of the National Academy of Sciences*, 111, 5616–5621.

Laurans, M., Hérault, B., Vieilledent, G. & Vincent, G. (2014). Vertical stratification reduces competition for light in dense tropical forests. *Forest Ecology and Management*, 329, 79–88.

Levionnois, S., Ziegler, C., Heuret, P., Jansen, S., Stahl, C., Calvet, E., *et al.* (2021). Is vulnerability segmentation at the leaf-stem transition a drought resistance mechanism? A theoretical test with a trait-based model for Neotropical canopy tree species. *Annals of Forest Science*, 78, 1–16.

Liang, J., Crowther, T.W., Picard, N., Wiser, S., Zhou, M., Alberti, G., *et al.* (2016). Positive biodiversity-productivity relationship predominant in global forests. *Science*, 354, 196.

Liang, J., Zhou, M., Tobin, P.C., McGuire, A.D. & Reich, P.B. (2015). Biodiversity influences plant productivity through niche-efficiency. *Proceedings of the National Academy of Sciences of the United States of America*, 112, 5738–5743.

Loreau, M. & de Mazancourt, C. (2013). Biodiversity and ecosystem stability: A synthesis of underlying mechanisms. *Ecology Letters*, 16, 106–115.

Luo, Y., Ho, C.L., Helliker, B.R. & Katifori, E. (2021). Leaf Water Storage and Robustness to Intermittent Drought: A Spatially Explicit Capacitive Model for Leaf Hydraulics. *Frontiers in Plant Science*, 12, 2269.

Machado, R., Loram-Lourenço, L., Farnese, F.S., Alves, R.D.F.B., de Sousa, L.F., Silva, F.G., et al. (2021). Where do leaf water leaks come from? Trade-offs underlying the variability in minimum conductance across tropical savanna species with contrasting growth strategies. *New Phytologist*, 229, 1415–1430.

Maréchaux, I., Bartlett, M.K., Sack, L., Baraloto, C., Engel, J., Joetzer, E. & Chave, J. (2015). Drought tolerance as predicted by leaf water potential at turgor loss point varies strongly across species within an Amazonian forest. *Functional Ecology*, 29, 1268–1277.

Maréchaux, I., Saint-André, L., Bartlett, M.K., Sack, L. & Chave, J. (2019). Leaf drought tolerance cannot be inferred from classic leaf traits in a tropical rainforest. *Journal of Ecology*, 108, 1030–1045.

Martin-StPaul, N.K., Delzon, S. & Cochard, H. (2017). Plant resistance to drought depends on timely stomatal closure. *Ecology Letters*, 20, 1437–1447.

Mas, E., Cochard, H., Deluigi, J., Didion-Gency, M., Martin-StPaul, N., Morcillo, L., et al. (2024). Interactions between beech and oak seedlings can modify the effects of hotter droughts and the onset of hydraulic failure. *New Phytologist*, 241, 1021–1034.

McElreath, R. (2020). *Statistical rethinking: A Bayesian course with examples in R and Stan*. CRC Press.

Meng, L., Chambers, J., Koven, C., Pastorello, G., Gimenez, B., Jardine, K., et al. (2022). Soil moisture thresholds explain a shift from light-limited to water-limited sap velocity in the Central Amazon during the 2015–16 El Niño drought. *Environmental Research Letters*, 17, 064023.

Mirabel, A., Hérault, B. & Marcon, E. (2020). Diverging taxonomic and functional trajectories following disturbance in a Neotropical forest. *Science of the Total Environment*, 720, 137397.

Moravie, M.A., Pascal, J.P. & Auger, P. (1997). Investigating canopy regeneration processes through individual-based spatial models: Application to a tropical rain forest. *Ecological Modelling*, 104, 241–260.

Moreno, M., Simioni, G., Cochard, H., Doussan, C., Guillemot, J., Decarsin, R., *et al.* (2023). Functional diversity reduces the risk of hydraulic failure in tree mixtures through hydraulic disconnection. *bioRxiv*, p. 2023.06.09.544345.

Moreno-Gutiérrez, C., Dawson, T.E., Nicolás, E. & Querejeta, J.I. (2012). Isotopes reveal contrasting water use strategies among coexisting plant species in a Mediterranean ecosystem. *New Phytologist*, 196, 489–496.

Morin, X., Fahse, L., Scherer-Lorenzen, M. & Bugmann, H. (2011). Tree species richness promotes productivity in temperate forests through strong complementarity between species. *Ecology Letters*, 14, 1211–1219.

Nemetschek, D., Derroire, G., Marcon, E., Aubry-Kientz, M., Auer, J., Badouard, V., *et al.* (2024). Climate anomalies and neighbourhood crowding interact in shaping tree growth in old-growth and selectively logged tropical forests. *Journal of Ecology*, 0.

Osnas, J.L.D., Lichstein, J.W., Reich, P.B. & Pacala, S.W. (2013). Global Leaf Trait Relationships: Mass, Area, and the Leaf Economics Spectrum. *Science*, 340, 741–744.

Pardos, M., del Río, M., Pretzsch, H., Jactel, H., Bielak, K., Bravo, F., *et al.* (2021). The greater resilience of mixed forests to drought mainly depends on their composition: Analysis along a climate gradient across Europe. *Forest Ecology and Management*, 481, 118687.

Pommerening, A. & Sánchez Meador, A.J. (2018). Tamm review: Tree interactions between myth and reality. *Forest Ecology and Management*, 424, 164–176.

Poorter, L., McDonald, I., Alarcón, A., Fichtler, E., Licona, J.C., Peña-Claros, M., *et al.* (2010). The importance of wood traits and hydraulic conductance for the performance and life history strategies of 42 rainforest tree species. *New Phytologist*, 185, 481–492.

R Core Team (2021). *R: A language and environment for statistical computing*. R Foundation for Statistical Computing, Vienna, Austria. URL <https://www.R-project.org/>, Vienna, Austria.

Reich, P.B. (2014). The world-wide ‘ fast – slow ’ plant economics spectrum: A traits manifesto. *Journal of Ecology*, 102, 275–301.

Rifai, S.W., Girardin, C.A., Berenguer, E., Del Aguila-Pasquel, J., Dahlsjö, C.A., Doughty, C.E., *et al.* (2018). ENSO Drives interannual variation of forest woody growth across the tropics. *Philosophical Transactions of the Royal Society B: Biological Sciences*, 373, 20170410.

Rodriguez-Dominguez, C.M., Buckley, T.N., Egea, G., de Cires, A., Hernandez-Santana, V., Martorell, S. & Diaz-Espejo, A. (2016). Most stomatal closure in woody species under moderate drought can be explained by stomatal responses to leaf turgor. *Plant, Cell & Environment*, 39, 2014–2026.

RStudio Team (2020). RStudio: Integrated Development Environment for R.

Scheidegger, Y., Saurer, M., Bahn, M. & Siegwolf, R. (2000). Linking stable oxygen and carbon isotopes with stomatal conductance and photosynthetic capacity: A conceptual model. *Oecologia*, 125, 350–357.

Shukla, P.R., Skea, J., Slade, R., Al Khourdajie, A., Van Diemen, R., McCollum, D., *et al.* (eds.) (2022). *IPCC: Climate Change 2022: Mitigation of Climate Change Working Group III to the Sixth Assessment Report of the Intergovernmental Panel on Climate Change*. Cambridge University Press, Cambridge, UK and New York, NY, USA.

Stan Development Team (2022). CmdStanR: the R interface to CmdStan.

- Tymen, B., Vincent, G., Courtois, E.A., Heurtebize, J., Dauzat, J., Marechaux, I. & Chave, J. (2017). Quantifying micro-environmental variation in tropical rainforest understory at landscape scale by combining airborne LiDAR scanning and a sensor network. *Annals of Forest Science*, 74, 32.
- Uriarte, M., Swenson, N.G., Chazdon, R.L., Comita, L.S., John Kress, W., Erickson, D., *et al.* (2010). Trait similarity, shared ancestry and the structure of neighbourhood interactions in a subtropical wet forest: implications for community assembly. *Ecology Letters*, 13, 1503–1514.
- Vile, D., Garnier, E., Shipley, B., Laurent, G., Navas, M.L., Roumet, C *et al.* (2005). Specific Leaf Area and Dry Matter Content Estimate Thickness in Laminar Leaves. *Annals of Botany*, 96, 1129–1136.
- Vleminckx, J., Fortunel, C., Valverde-Barrantes, O., Timothy Paine, C.E., Engel, J., Petronelli, P., *et al.* (2021). Resolving whole-plant economics from leaf, stem and root traits of 1467 Amazonian tree species. *Oikos*, 130, 1193– 1208.
- Wagner, F., Rossi, V., Baraloto, C., Bonal, D., Stahl, C. & Hérault, B. (2014). Are commonly measured functional traits involved in tropical tree responses to climate? *International Journal of Ecology*, 2014, 389409.
- Wagner, F.H., Hérault, B., Bonal, D., Stahl, C., Anderson, L.O., Baker, T.R., *et al.* (2016). Climate seasonality limits leaf carbon assimilation and wood productivity in tropical forests. *Biogeosciences*, 13, 2537–2562.
- Westoby, M., Falster, D.S., Moles, A.T., Vesk, P.A. & Wright, I.J. (2002). Plant ecological strategies: Some leading dimensions of variation between species. *Annual Review of Ecology and Systematics*, 33, 125–159.
- Wickham, H., Averick, M., Bryan, J., Chang, W., McGowan, L.D., François, R., *et al.* (2019). Welcome to the tidyverse. *Journal of Open Source Software*, 4, 1686.
- Wright, A.J. (2024). Plant–plant interactions can mitigate (or exacerbate) hot drought impacts. *New Phytologist*, 241, 955–957.

Wright, I.J., Dong, N., Maire, V., Prentice, I.C., Westoby, M., Díaz, S., *et al.* (2017). Global climatic drivers of leaf size. *Science*, 357, 917–921.

Wright, I.J., Reich, P.B., Westoby, M., Ackerly, D.D., Baruch, Z., Bongers, F., *et al.* (2004). The worldwide leaf economics spectrum. *Nature*, 428, 821–827.

Yu, W., Albert, G., Rosenbaum, B., Schnabel, F., Bruelheide, H., Connolly, J., *et al.* (2024). Systematic distributions of interaction strengths across tree interaction networks yield positive diversity–productivity relationships. *Ecology Letters*, 27, e14338.

Zhang, S., Landuyt, D., Verheyen, K. & De Frenne, P. (2022). Tree species mixing can amplify microclimate offsets in young forest plantations. *Journal of Applied Ecology*, 59, 1428–1439.

Ziegler, C., Coste, S., Stahl, C., Delzon, S., Levionnois, S., Cazal, J., *et al.* (2019). Large hydraulic safety margins protect Neotropical canopy rainforest tree species against hydraulic failure during drought. *Annals of Forest Science*, 76, 115.